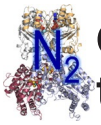

Chimeric Interaction of Nitrogenase-Like Reductases with the MoFe Protein of Nitrogenase

Jan Jasper,[a] José V. Ramos,[b] Christian Trncik,[c] Dieter Jahn,[a] Oliver Einsle,[c] Gunhild Layer,[b] and Jürgen Moser*[a]

The engineering of transgenic organisms with the ability to fix nitrogen is an attractive possibility. However, oxygen sensitivity of nitrogenase, mainly conferred by the reductase component $(NifH)_2$, is an imminent problem. Nitrogenase-like enzymes involved in coenzyme F_{430} and chlorophyll biosynthesis utilize the highly homologous reductases $(CfbC)_2$ and $(ChlL)_2$, respectively. Chimeric protein–protein interactions of these reductases with the catalytic component of nitrogenase (MoFe protein) did not support nitrogenase activity. Nucleotide-dependent association and dissociation of these complexes was investigated, but $(CfbC)_2$ and wild-type $(ChlL)_2$ showed no modulation of the binding affinity. By contrast, the interaction between the $(ChlL)_2$ mutant Y127S and the MoFe protein was markedly increased in the presence of ATP (or ATP analogues) and reduced in the ADP state. Upon formation of the octameric $(ChlL)_2MoFe(ChlL)_2$ complex, the ATPase activity of this variant is triggered, as seen in the homologous nitrogenase system. Thus, the described reductase(s) might be an attractive tool for further elucidation of the diverse functions of $(NifH)_2$ and the rational design of a more robust reductase.

Introduction

The complex metalloenzyme nitrogenase is responsible for the fixation of atmospheric dinitrogen, which is a crucial process in the global nitrogen cycle. This enzymatic conversion requires significant energy input for the addition of electrons and protons to dinitrogen under ambient conditions to yield two molecules of ammonia.[1] Industrial reduction of dinitrogen by the Haber–Bosch process occurs at about 450 °C and >200 atm and accounts for the consumption of approximately 1.4% of the global energy demand.[2] The best studied molybdenum nitrogenase of *Azotobacter vinelandii* consists of two components, an ATP-dependent reductase $(NifH)_2$, which is commonly known as the Fe protein, and the catalytic component named the molybdenum–iron (MoFe) protein (Figure 1).[3] Homodimeric $(NifH)_2$ is bridged by a single inter-subunit [4Fe–4S] cluster and contains one ATP-binding site per NifH subunit. The heterotetrameric MoFe protein $(NifD/NifK)_2$ has two unique metal clusters per (NifD/NifK)-protomer: the P-cluster is located at the NifD/NifK subunit interface and the FeMoco cluster (or the M-cluster) is buried within the NifD subunit (Figure 1).[4,5] Biochemical and structural investigations revealed that the $(NifH)_2$ function is based on a dynamic switch mechanism linking ATP hydrolysis to substantial conformational changes.[4,6–10] For catalytic dinitrogen reduction, $(NifH)_2$ transiently forms a complex with the MoFe protein. This complex possesses an octameric architecture, $(NifH)_2(NifD/NifK)_2(NifH)_2$, and facilitates the transfer of electrons from the [4Fe–4S] cluster of $(NifH)_2$ to the P-cluster of $(NifD/NifK)_2$. These electrons are then further delivered and eventually accumulated on FeMoco, which is the site of nitrogen fixation.[5,11] A schematic model for the electron-transfer processes, and dynamic association and dissociation during ATP-driven nitrogenase catalysis is depicted in Figure 2. Several rounds of this catalytic cycle are required to supply the electrons required for nitrogen reduction.

Tremendous progress in understanding biological dinitrogen fixation was made in recent years.[5,9,11–16] Among other things, the key steps for the maturation of the sophisticated metallocenters have been deciphered, which might be an important step towards the design of plants or plant-associated organisms with improved nitrogen-fixing ability. The present state of transgenic nitrogenase engineering has been recently summarized.[17] In all cases, the oxygen sensitivity of nitrogenase, mainly conferred by the reductase component $(NifH)_2$, represents a difficult problem. In vivo, the *A. vinelandii* nitrogenase is protected from oxidative damage by binding the nitroge-

[a] J. Jasper, Prof. Dr. D. Jahn, Dr. J. Moser
Institut für Mikrobiologie, Technische Universität Braunschweig
Spielmannstrasse 7, 38106 Braunschweig (Germany)
E-mail: j.moser@tu-bs.de

[b] J. V. Ramos, Prof. Dr. G. Layer
Institut für Pharmazeutische Wissenschaften
Pharmazeutische Biologie und Biotechnologie
Albert-Ludwigs-Universität Freiburg
Stefan-Meier-Str. 19, 79104 Freiburg (Germany)

[c] C. Trncik, Prof. Dr. O. Einsle
Institut für Biochemie, Albert-Ludwigs-Universität Freiburg
Albertstrasse 21, 79104 Freiburg (Germany)

Supporting information and the ORCID identification numbers for the authors of this article can be found under https://doi.org/10.1002/cbic.201900759.

This article is part of a Special Issue on Nitrogenases and Homologous Systems.

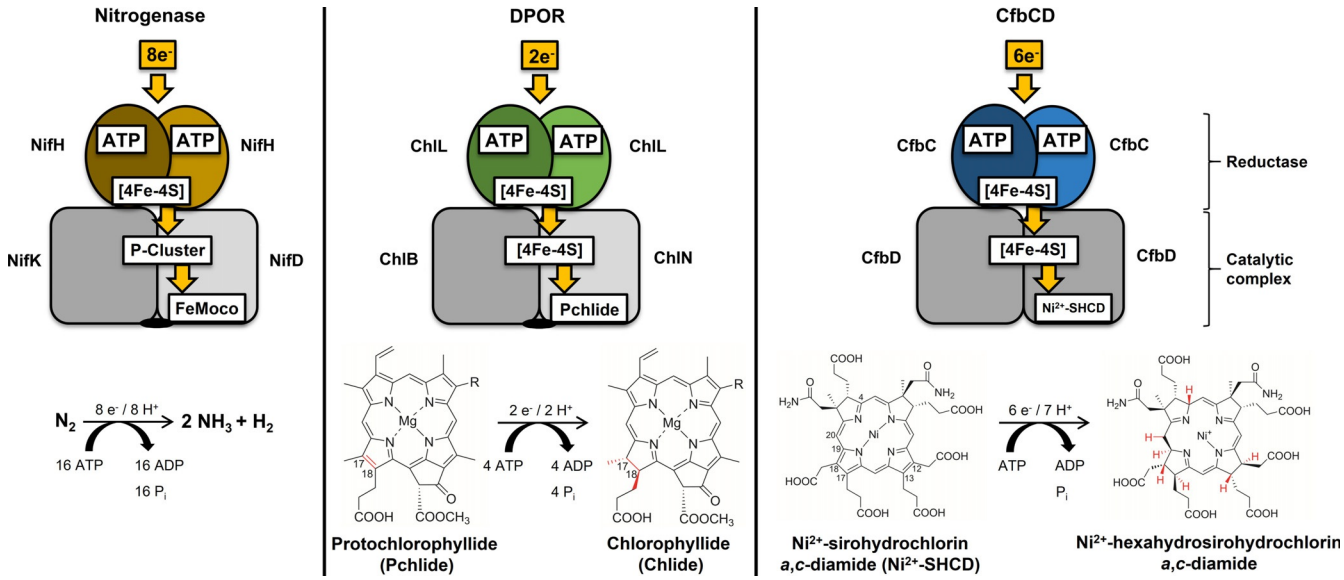

Figure 1. Schematic representation of transient complexes of nitrogenase, dark operative protochlorophyllide oxidoreductase (DPOR), and CfbCD. Nitrogenase and DPOR share an octameric protein architecture (only one half-octamer is shown; the appropriate twofold symmetry of the overall complex is indicated by a spindle). CfbCD forms a tetrameric $(CfbC)_2(CfbD)_2$ complex (see the Results and Discussion). Homologous ATP-dependent reductases $(NifH)_2$, $(ChlL)_2$, and $(CfbC)_2$ are highlighted in brown, green, and blue, respectively. Related catalytic components are depicted in gray. Nitrogenase catalyzes the biological reduction of dinitrogen to ammonia. DPOR drives the two-electron reduction of the conjugated ring system of protochlorophyllide (Pchlide) to chlorophyllide (Chlide; highlighted in red; R is either ethyl or vinyl). CfbCD catalyzes the six-electron reduction of Ni^{2+}-sirohydrochlorin *a*,*c*-diamide (Ni^{2+}-SHCD) to Ni^{2+}-hexahydrosirohydrochlorin *a*,*c*-diamide (introduced protons colored red). Electron transfer through redox-active metallocenters ([4Fe–4S] cluster, [8Fe–7S] cluster termed P-cluster, and $MoFe_7S_9C$-homocitrate named FeMoco) is schematically indicated by arrows.

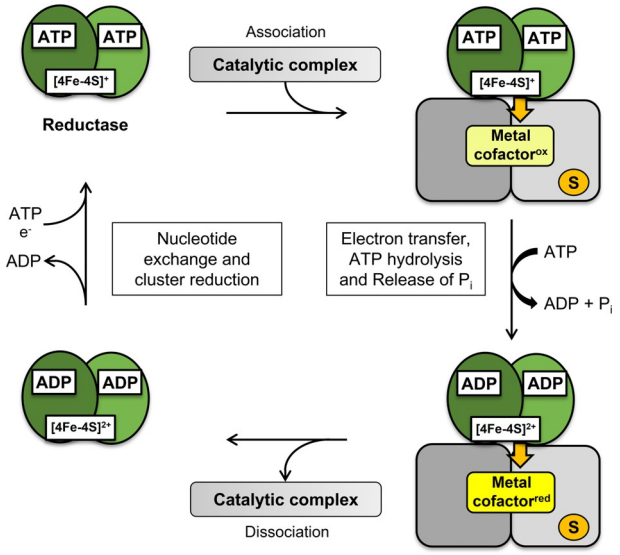

Figure 2. Schematic representation of the catalytic cycle of nitrogenase and DPOR. Electron-transfer processes and the dynamic interaction of reductases $(NifH)_2$ or $(ChlL)_2$, in green, with the related catalytic subunits MoFe or $(ChlN/ChlB)_2$, in gray, is indicated. The reductase in the ATP-bound "on state" transiently associates with the catalytic complex, thereby facilitating electron transfer from the reduced $[4Fe–4S]^+$ cluster to the metal cofactor of the catalytic subunit (yellow and bright yellow, respectively). ATP hydrolysis and the release of P_i leads to the ADP-bound "off state" of the reductase, which triggers the dissociation of the overall complex. Nucleotide exchange and the re-reduction of the $[4Fe–4S]^{2+}$ cluster is required for the subsequent redox catalytic cycle. Consecutive single-electron reductions provide eight or two electrons, which are required for the substrate (S) conversion of nitrogenase or DPOR.

nase-protective protein FeSII, but the enzyme is converted into a temporarily inactivated state.[18,19] Accordingly, the identification or, alternatively, the design of a more "robust" nitrogenase reductase represents an important goal for subsequent synthetic biology approaches. Towards this goal, nitrogenase-like enzymes involved in cofactor F_{430} and chlorophyll biosynthesis can be considered. These orthologous two-component enzymes rely on a reductase facilitating ATP-driven electron transfer onto their respective catalytic subunits by close analogy to $(NifH)_2$. The related catalytic complexes contain more simple metal cofactors in the form of [4Fe–4S] clusters.

DPOR

The biosynthesis of chlorophylls and bacteriochlorophylls involves the reduction of the C17=C18 bond of the conjugated ring system of Pchlide by DPOR, which results in the formation of Chlide (Figure 1).[20] DPOR consists of the ATP-dependent reductase, $(ChlL)_2$, and the catalytic unit, $(ChlN/ChlB)_2$, both sharing a substantial degree of structural and amino acid sequence identity with nitrogenase (compare sequence alignment in Figure S1 in the Supporting Information). $(ChlL)_2$ carries a bridging inter-subunit [4Fe–4S] cluster and contains one ATP-binding site per ChlL subunit.

Biochemical and structural investigations identified a dynamic switch mechanism for $(ChlL)_2$, in close analogy to that of $(NifH)_2$. ATP hydrolysis in $(ChlL)_2$ is linked to conformational changes, which have been experimentally characterized as follows. The on state of $(ChlL)_2$ is induced in the presence of ATP (or ATP analogues) and possesses a high affinity for (ChlN/

$ChlB)_2$. ATP analogues, such as ADP·AlF_3 or β,γ-imidoadenosine 5′-triphosphate (AMP-PNP), have been used to efficiently "freeze" the transient interaction of nitrogenase and DPOR for subsequent biochemical and structural investigations, respectively.[21,22] The "off state" conformation of $(ChlL)_2$ in the presence of ADP revealed a significantly lower affinity for (ChlN/$ChlB)_2$ and led to the dissociation of the overall complex. Parallelism for the overall redox catalytic cycle of reductases $(ChlL)_2$ and $(NifH)_2$ was demonstrated.[23] This nucleotide-dependent dynamic switch mechanism is depicted in Figure 2. Structural investigations revealed a detailed picture of each of the two different states (Figure 3). The three-dimensional structure of the sole DPOR reductase (from *Rhodobacter sphaeroides*)[24] and of the isolated catalytic complex[25,26] (from *Thermosynechococcus elongatus* or *Rhodobacter capsulatus*) revealed the main principles of nucleotide and substrate recognition in the off state of DPOR catalysis. For trapping of the on state, the ternary DPOR complex is quantitatively assembled in the presence of ADP·AlF_3, which is a putative transition state analogue of ATP hydrolysis.[23] The structure of the overall octameric complex revealed perfect twofold symmetry.[22] Accordingly, binding of a sole $(ChlL)_2$ dimer per (ChlN/ChlB) half-tetramer is depicted in Figures 1 and 3.

On the basis of the noncomplexed structure, theoretical rigid-body docking of $(ChlL)_2$ would result in a distance of about 17.3 Å between both iron–sulfur centers of DPOR. However, the X-ray structure of the ternary complex revealed a cluster arrangement with both [4Fe–4S] centers in a 3.2 Å closer position (14.1 Å, closest atom to atom distance). Clearly, electron transfer of $(ChlL)_2$ is mediated by the spatial rearrangement of the redox active [4Fe–4S] center (Figure 3A, B). Upon DPOR ternary complex formation, conformational rearrangements cause a more compact quaternary $(ChlL)_2$ structure. These movements comprise a rotation of each ChlL monomer with its bound nucleotide cofactor towards the conserved dimer interface of $(ChlL)_2$ (compare movement of respective adenine bases in Figure 3A, B). The inter-subunit rearrangement is triggered by highly conserved interface residues, in response to a change of the ADP-bound to the ATP-bound nucleotide state. Amino acid residues Asp155* and Lys37*, provided by the neighboring ChlL monomer, were proposed as key residues for the hydrolysis of ATP. Superposition of the off- and on-state conformations of $(ChlL)_2$ revealed peptide segments undergoing significant Cα-rearrangements. These key residues of the dynamic switch region comprise the switch I region (Cys65–Thr72), which communicates the nucleotide state to the docking loop (Pro118–Tyr127). The second sequence, called the switch II region (Leu153–Cys158), includes the above-mentioned residue, Asp155, and one ligand of the [4Fe–4S] cluster of $(ChlL)_2$. Peptide regions Met79–Glu96 and Pro118–Tyr127, including the second cluster ligand Cys124, are responsible for the dynamic repositioning of the [4Fe–4S] cluster upon ternary complex formation (Figure 3A). Structural comparison of $(NifH)_2$ of nitrogenase in the off and on states (e.g., PDB IDs: 1FP6 and 1N2C) indicated strong parallelism for the dynamic switch mechanism of $(ChlL)_2$ and $(NifH)_2$,[22] as indicated by almost perfect conservation of the switch I region (Gly37–Thr45) and of the switch II region (Asp125–Phe135; NifH numbering, cf. Figure S1). This was further illustrated by the pairwise structural comparison of $(ChlL)_2$ and $(NifH)_2$, which revealed a structural root-mean-square deviation of only 1.7 and 1.1 Å for the off- and on-state conformations, respectively.[27]

Ni^{2+}-SHCD reductase CfbCD

The nitrogenase-like genes *cfbC* and *cfbD* (formerly denoted as *nflH* and *nflD*, nfl stands for nitrogen fixation-like) are present

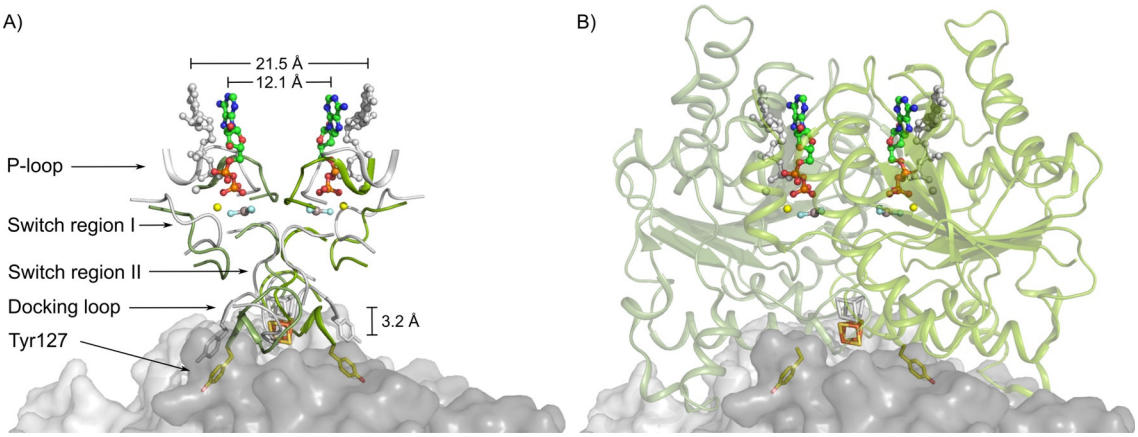

Figure 3. The dynamic switch mechanism of the $(ChlL)_2$ reductase of DPOR. A) Superposition of the on-state conformation of $(ChlL)_2$ in the ADP·AlF_3-stablized complex (green; PDB ID: 2YNM) and the off-state conformation, as observed in the ADP-bound state (gray; PDB ID: 3FWY). Nucleotide-dependent conformational rearrangements trigger the affinity of $(ChlL)_2$ for the catalytic complex, $(ChlN/ChlB)_2$ (bright gray and gray surface). Movement of the [4Fe–4S] cluster of $(ChlL)_2$ by 3.2 Å upon $(ChlL)_2(ChlN/ChlB)_2(ChlL)_2$ complex formation is indicated. Only peptide segments undergoing large Cα-rearrangements are shown: Gly36–Ser43 (P-loop), Cys65–Thr72 (switch I), Leu153–Cys158 (switch II), and Pro118–Tyr127 (docking loop). Movement of each ChlL monomer towards the dimer interface of $(ChlL)_2$ becomes evident by a 9.4 Å decrease in the distance between the adenine bases in the off state (gray ball and sticks) and the on state (ADP·AlF_3 colored ball and sticks, Mg^{2+} yellow). B) Docking of the overall $(ChlL)_2$ reductase to $(ChlN/ChlB)_2$, with the same colors as those in A). The spatial position of residue Tyr127 (yellow sticks) at the docking face is indicated (A and B). PyMOL was used to generate this figure.[27]

in all methanogenic archaea.[28–30] The corresponding nitrogenase-like two-component system CfbCD is involved in coenzyme F_{430} biosynthesis by catalyzing the reduction of the intermediate Ni^{2+}-SHCD to the tetrahydrocorphinat Ni^{2+}-hexahydrosirohydrochlorin *a,c*-diamide, which is a reaction that requires the input of $6e^-$ and $7H^+$ (Figure 1).[31,32] The ATP-dependent reductase $(CfbC)_2$ shares a substantial degree of sequence conservation with $(NifH)_2$ and $(ChlL)_2$. The homodimeric protein carries a [4Fe–4S] cluster, which exhibits EPR signals that change upon the addition of MgATP or MgADP, in line with a nucleotide-dependent dynamic switch mechanism for electron transfer onto the catalytic component, $(CfbD)_2$, which also carries a [4Fe–4S] cluster. When $(CfbC)_2$ and $(CfbD)_2$, both dithionite-reduced, were mixed, the intensity of the EPR signal of the $(CfbD)_2$ [4Fe–4S] cluster increased upon the addition of MgATP, in line with the proposed nucleotide-dependent electron transfer from $(CfbC)_2$ to $(CfbD)_2$.[31] Even in the absence of related three-dimensional protein structures, the conservation of the switch I region (Gly39–Ser47), of the docking loop (Gly88–Ala104), and of the switch II region (Asp125–Phe135, *Methanosarcina barkeri* numbering) and both proposed [4Fe–4S] cluster ligands (Figure S1) indicates a catalytic redox cycle of $(CfbC)_2$, which is closely related to that of nitrogenase reductase. From an evolutionary perspective, the CfbCD system was suggested to be a "simplified" ancestor lying basal in the phylogenetic tree between nitrogenase and DPOR.[33]

To date, $(NifH)_2$ is the only reductase of the MoFe protein that supports dinitrogen reduction. However, dinitrogen reducing activity has been demonstrated by using heterologous nitrogenase components.[34] Inactive heterologous nitrogenase complexes have also been studied, and thus, allow for a deeper understanding of nitrogenase.[35–37] For the DPOR system, related experiments in the presence of heterologous combinations of reductase and catalytic components also demonstrated DPOR activity. Furthermore, it was shown that chimeric enzyme systems between nitrogenase-like enzymes could be formed.[38] The cyanobacterium *Prochlorococcus marinus* performs oxygenic photosynthesis, which might indicate that the reductase $(ChlL)_2$ of this organism possesses an improved tolerance towards molecular oxygen.

Here, we investigate the chimeric protein–protein interaction of the nitrogenase-like reductases $(CfbC)_2$ or $(ChlL)_2$ with the MoFe protein. Nucleotide-dependent protein complex formation and the reductant-independent ATP-hydrolysis activity of wild-type and mutant proteins are investigated as an initial step towards the engineering of an alternative nitrogenase reductase.

Results and Discussion

$(CfbC)_2$ and $(CfbD)_2$ form a tight complex

From theoretical sequence analyses, $(CfbC)_2$ was considered to be an ancestral reductase from which the related nitrogenase and DPOR proteins evolved. However, details of the interplay between $(CfbC)_2$ and $(CfbD)_2$ have not been investigated, so far. Accordingly, the protein–protein interaction of the dimeric components was analyzed by using two different experimental strategies.

In the first approach, complex formation between $(CfbC)_2$ and $(CfbD)_2$ was analyzed by ultrafiltration using filter units with a molecular-weight cutoff of 100 kDa. After mixing the two components and filtration (see the Experimental Section), the single components were expected to be present in the filtrate, whereas the potential complex should be retained by the filter in the >100 kDa fraction, which was analyzed by means of SDS-PAGE. As shown in Figure 4A, as the mixture passed through the ultrafiltration unit, both proteins, $(CfbC)_2$ and $(CfbD)_2$, were retained by the filter, which indicated complex formation independent of the presence or absence of the ATP analogue AMP-PNP (Figure 4A, lanes 1 and 2). The same result was obtained with protein mixtures containing ADP or ATP (not shown). In contrast, the single $(CfbC)_2$ or $(CfbD)_2$ proteins were not retained by the filter, as expected (Figure 4A, lanes 3 and 4). Since these first experiments suggested an interaction between $(CfbC)_2$ and $(CfbD)_2$, the potential protein complex was further analyzed for its stability and oligomeric architecture by means of gel filtration chromatography. For this purpose, $(CfbC)_2$ (15 μM) and $(CfbD)_2$ (17.5 μM) were mixed, and the sample was analyzed by using a Superdex 200 5/150 GL column. As shown in Figure 4B, the two proteins eluted together as a complex with a native molecular weight of about 135 000 in good agreement with an overall tetrameric $(CfbC)_2(CfbD)_2$ protein architecture (see Figure 1). Again, complex formation and stability, as analyzed by means of gel filtration, were identical for samples with or without added nucleotides (Figure S2). Overall, these findings suggest that $(CfbC)_2$ and $(CfbD)_2$ form a 1:1 complex, and we conclude that the interaction between $(CfbC)_2$ and $(CfbD)_2$ is not modulated in the presence of different nucleotides.

Interestingly, nucleotide-independent interactions between $(NifH)_2$ and MoFe protein from *A. vinelandii* were observed previously and described as "encounter complexes", representing an initial docking geometry between the two components.[39] In our case, it is not possible to tell whether the observed $(CfbC)_2(CfbD)_2$ complex represents an encounter complex or the catalytically active "sitting atop" complex due to the lack of structural information. Nevertheless, the comparatively tight binding of $(CfbC)_2$ might be beneficial to preserve the labile [4Fe–4S] cluster of the reductase. Accordingly, $(CfbC)_2$ was further investigated as a potential interaction partner of the MoFe protein of nitrogenase.

$(CfbC)_2$ and MoFe form a weak complex

The chimeric interaction between $(CfbC)_2$ and MoFe was investigated by using the same approaches as those described above. With the established ultrafiltration methodology, an interaction between $(CfbC)_2$ and MoFe was observed. As indicated in lanes 1–4 of Figure 4C, $(CfbC)_2$ was retained by the membrane, as a result of its interaction with MoFe, whereas in control experiments the unbound reductase was exclusively found in the filtrate (cf. Figure 4A). Almost identical results were ob-

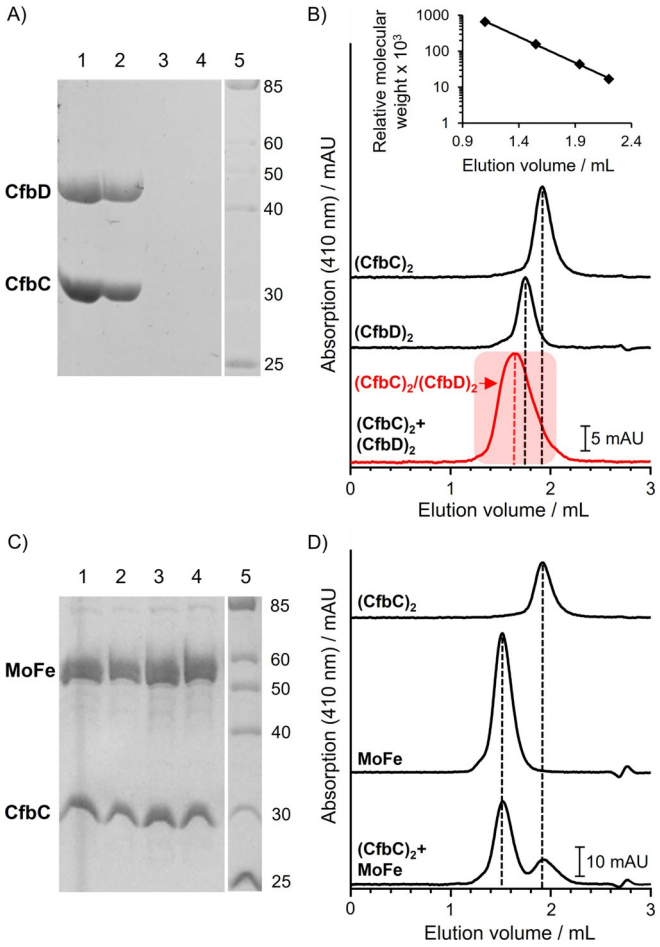

Figure 4. Homologous and heterologous interactions of $(CfbC)_2$. A) SDS-PAGE analysis of ultrafiltration experiments, indicating homologous complex formation between $(CfbC)_2$ and $(CfbD)_2$. Interaction of $(CfbC)_2$ with $(CfbD)_2$ was analyzed by using an ultrafiltration membrane with a molecular-weight cutoff of 100 kDa; retained protein fractions were analyzed by means of SDS-PAGE. $(CfbC)_2+(CfbD)_2$ (lane 1) and $(CfbC)_2+(CfbD)_2$ in the presence of AMP–PNP (lane 2) indicated complex formation. Control experiments in the presence of AMP–PNP showed that individual components, $(CfbC)_2$ and $(CfbD)_2$, were not retained by the membrane (lanes 3 and 4); lane 5: molecular-weight marker, relative molecular masses (×1000) are indicated. B) Gel permeation chromatography of $(CfbC)_2$, $(CfbD)_2$, and the $(CfbC)_2(CfbD)_2$ complex. The native molecular weight was analyzed on a Superdex 200 5/150GL column previously calibrated (insert) by using the protein standards thyroglobulin (M_r = 670 000), γ-globulin (M_r = 158 000), ovalbumin (M_r = 44 000), and myoglobin (M_r = 17 000). C) Ultrafiltration experiments (as detailed in A) containing $(CfbC)_2$ and MoFe, indicating heterologous complex formation. Lane 1: +AMP–PNP; lane 2: +ADP; lane 3: +ATP; lane 4: without nucleotides; lane 5: molecular-weight marker, relative molecular masses (×1000) are indicated. D) Gel permeation chromatography of $(CfbC)_2$, MoFe, and a $(CfbC)_2$/MoFe sample. No heterologous complex was detected.

served in the presence of 1.5 mM ATP, ADP, or AMP-PNP. These results indicate that the apparent interaction between $(CfbC)_2$ and MoFe is not modulated by the presence of different nucleotides, in agreement with the results for the homologous $(CfbC)_2(CfbD)_2$ complex. Gel filtration experiments with a threefold excess of $(CfbC)_2$, relative to the MoFe protein in the absence or presence of 1.5 mM ATP, ADP, or AMP–PNP, did not reveal the formation of a stable chimeric complex (Figures 4D and S2). Apparently, the interaction between $(CfbC)_2$ and MoFe is not as strong as that for the homologous system, and the affinity between the heterologous components is not increased by the presence of nucleotides. Finally, standard nitrogenase activity experiments did not reveal enzymatic conversion of dinitrogen or azide in the presence of $(CfbC)_2$, MoFe, and dithionite.[40] Analysis of Ti^{III} citrate oxidation did not show electron transfer through the chimeric complex.[41]

Trapping the chimeric $(ChlL)_2MoFe(ChlL)_2$ complex

Comparison of nitrogenase and DPOR docking faces on the basis of X-ray crystallographic structures suggested that $(ChlL)_2$ did not fit as a binding partner of the MoFe protein.[22] However, conformational protein dynamics,[42] or even the involvement of varying docking geometries in the time course of nitrogenase catalysis, have to be considered.[10] To study the potential interaction of $(ChlL)_2$ and MoFe protein, glutathione S-transferase (GST)-tagged $(ChlL)_2$ from *P. marinus* was immobilized on Protino Glutathione Agarose and subsequently incubated with the purified MoFe protein in the presence of 2 mM $AlCl_3$, 10 mM MgADP, and 50 mM NaF, as recently described for trapping of the homologous DPOR complex.[23] After a washing step, the bait protein was liberated from the affinity matrix by means of PreScission protease cleavage of the GST-ChlL fusion. As indicated in the SDS-PAGE results shown in Figure 5 (cf. lanes 2–4), ChlL, with a calculated molecular mass of 32 395 Da, coeluted in the presence of MoFe (subunits NifD and NifK, 55 289 and 59 460 Da, respectively). The native molecular weight of the resulting protein complex was further characterized by means of size-exclusion chromatography under anaerobic conditions. A relative molecular weight of 355 000 (elution volume 55.6 mL) was determined (Figure 5), and SDS-PAGE analysis of the fractionated complex (Figure 5, lane 5) revealed a ratio of 2.1 mol of the $(ChlL)_2$ dimer per mol of the MoFe tetramer. From these findings, a chimeric octamer with a stoichiometry of $(ChlL)_2MoFe(ChlL)_2$ was proposed (calculated molecular mass 359 078 Da).

These results might indicate the formation of a chimeric complex with the same octamer architecture as that observed for the homologous DPOR and nitrogenase complexes. However, nitrogenase catalysis was not supported by the chimeric complex (dinitrogen or azide conversion, Ti^{III} citrate oxidation).

Nucleotide-dependent interaction of $(ChlL)_2$ and MoFe

Nucleotide-dependent affinity changes are of central importance for the dynamic switch mechanism of nitrogenase. The immobilized GST-tagged $(ChlL)_2$ protein (on Protino Glutathione Agarose) facilitates the direct investigation of the interaction with the MoFe protein in response to different nucleotides under anaerobic conditions. Identical aliquots containing immobilized $(ChlL)_2$ were processed in the presence of 10 mM ATP, 10 mM ADP, or 1.5 mM AMP-PMP. Stoichiometric amounts (2.5 nmol) of MoFe were added and, after incubation and washing, the trapped proteins were liberated from the affinity matrix and analyzed by means of SDS-PAGE. The ratio of MoFe versus $(ChlL)_2$ was calculated based on densitometry measure-

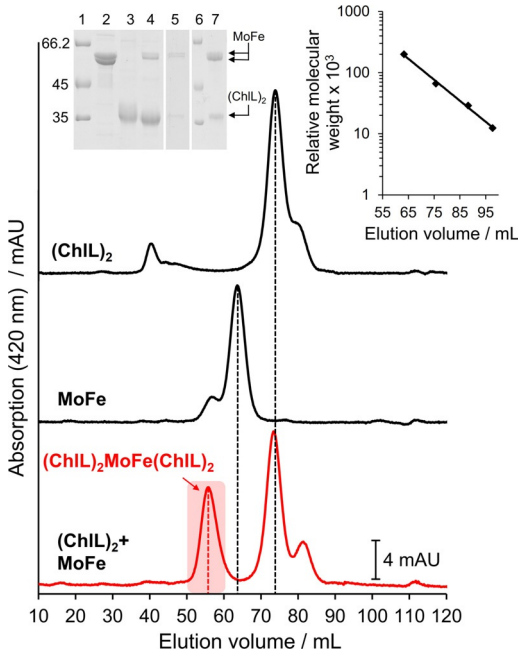

Figure 5. Assembly and native molecular-weight determination of the chimeric $(ChlL)_2MoFe(ChlL)_2$ complex. GST-tagged $(ChlL)_2$ was immobilized and the chimeric complex with MoFe was assembled in the presence of MgADP, $AlCl_3$, and NaF. The resulting complex was liberated by PreScission protease cleavage. The native molecular weights of the MoFe protein, $(ChlL)_2$, and the chimeric complex (red) were analyzed on a HiLoad Superdex 200 16/60 column previously calibrated (right inset) by using protein standards β-amylase (M_r = 200 000), albumin (M_r = 66 000), carbonic anhydrase (M_r = 29 000), and cytochrome *c* (M_r = 12 400). SDS-PAGE (left inset): Lanes 1 and 6: molecular-weight marker, relative molecular masses (×1000) are indicated; lane 2: purified MoFe protein; lane 3: purified $(ChlL)_2$; lane 4: elution of the chimeric complex after protease cleavage; lane 5: fractions of the chimeric complex, as obtained by means of size-exclusion chromatography (elution volume 55–60 mL); and lane 7: identical sample concentrated by ultrafiltration.

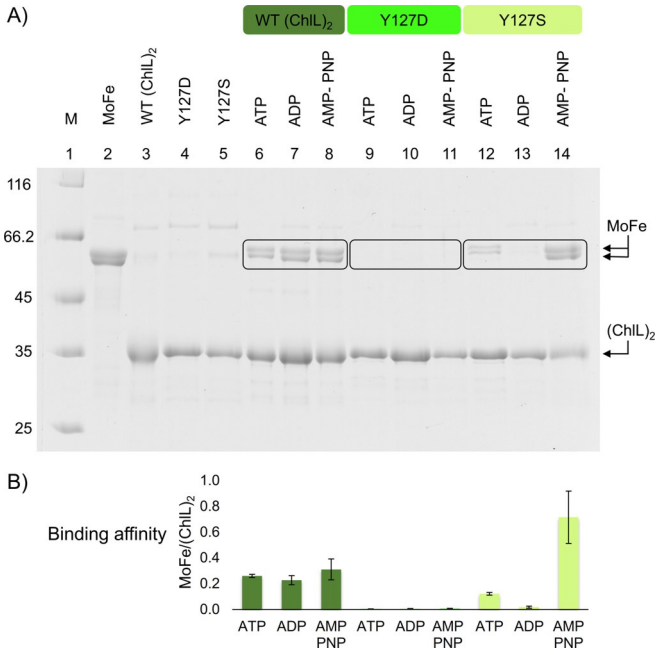

Figure 6. Nucleotide-dependent interaction of $(ChlL)_2$ proteins and MoFe. A) Protein–protein interactions of the immobilized reductase $(ChlL)_2$ (or variants Y127D and Y127S), with MoFe in the presence of ATP, ADP, and AMP-PMP were analyzed by means of SDS-PAGE. Lane 1: molecular-weight marker, relative molecular masses (×1000) are indicated; lanes 2–5: purified proteins MoFe, $(ChlL)_2$, $(ChlL)_2$ Y127D, and $(ChlL)_2$ Y127S; lanes 6–8, 9–11, and 12–14: interaction of $(ChlL)_2$, $(ChlL)_2$ Y127D, and $(ChlL)_2$ Y127S with MoFe in the presence of ATP, ADP, or AMP-PNP, respectively. B) Protein quantification using GelQuant.NET software to calculate the MoFe/$(ChlL)_2$ ratio of binding experiments.

ments after SDS-PAGE analyses. As indicated in Figure 6 A, lanes 6–8, $(ChlL)_2$ revealed an almost identical affinity for MoFe in the presence of ATP, ADP, and AMP-PMP. Clearly, the interaction is not affected by different nucleotides, which might explain the lack of ability for $(ChlL)_2$ to act as a nitrogenase reductase, as also observed for $(CfbC)_2$.

Tuning nucleotide-dependent interaction by site-directed mutagenesis

Structural investigations revealed the involvement of 35 ChlL or 34 NifH residues at the docking face of DPOR or nitrogenase, respectively (cf. Figure S1).[22] To examine the importance of specific residues for docking, we generated two variant $(ChlL)_2$ reductases containing a set of 27 or 8 mutagenized docking residues, with the aim of converting $(ChlL)_2$ into an artificial nitrogenase reductase. However, the recombinant proteins were purified as huge aggregates, as determined by means of gel filtration. Accordingly, these variants did not support nitrogenase activity and were not used in further interaction studies.

A more conservative approach was pursued that focused on the influence of single amino acid exchanges. The central importance of Tyr127 at the DPOR docking face was already exemplified.[38] Investigation of the nucleotide-dependent interplay of the $(ChlL)_2$ variant Y127D revealed a complete loss of MoFe interaction (Figure 6, lanes 9–11). Clearly, the negatively charged aspartate residue at the protein surface completely abolishes the chimeric interaction with MoFe. This might indicate that the docking face of the proposed $(ChlL)_2MoFe(ChlL)_2$ complex and of the homologous DPOR complex are spatially related. As expected, nitrogenase catalysis was not supported by $(ChlL)_2$ variant Y127D.

Exchange of Tyr127 into serine revealed a completely different result (Figure 6, lanes 12–14). In interaction studies, mutant Y127S showed a low binding affinity in the presence of ADP, as indicated by the binding of 0.02 mol MoFe per mol $(ChlL)_2$. This value was substantially increased to 0.12 in the presence of ATP and a maximum of 0.71 mol MoFe per mol $(ChlL)_2$ was observed in the presence of the ATP analogue AMP-PNP. These findings clearly indicate that the Y127S variant is able to modulate the artificial interaction with MoFe similarly to that described for the homologous nitrogenase and DPOR systems.[10,22,43,44] Despite the dynamic protein–protein interaction, variant Y127S was not active in terms of dinitrogen or azide reduction or the oxidation of Ti^{III} citrate.

Nitrogenase or DPOR catalysis can be followed not only by measuring ultimate substrate reduction. The ATP hydrolyzing activity of the respective reductase components has been effi-

ciently used to investigate initial stages of the sophisticated catalytic cycle of both systems. Reductant-independent ATPase activity has been demonstrated for nitrogenase. This enzymatic activity was substantially enhanced upon addition of the MoFe protein.[45–49] A related stimulation of the ATPase activity of $(ChlL)_2$ in the presence of $(ChlN/ChlB)_2$ was also demonstrated for the DPOR system.[23] Clearly, the triggering of the ATPase activity upon ternary complex formation is of central importance for DPOR and nitrogenase catalysis. Concerning the interplay of $(ChlL)_2$ and MoFe, we further investigated the ATPase activity of wild-type and mutant $(ChlL)_2$ proteins in the absence and presence of MoFe.

Reductant-independent ATPase activity of variant $(ChlL)_2$ proteins

The wild-type reductase $(ChlL)_2$ revealed a basal ATPase activity of 0.3 nmol mg^{-1} min^{-1} under the employed in vitro conditions (Figure 7). This value was increased to 0.6 nmol mg^{-1} min^{-1} in the presence of $(ChlN/ChlB)_2$. Such subunit cross talk was also observed for the chimeric system. In the presence of MoFe, the ATPase activity of $(ChlL)_2$ was substantially increased to a value of 16.0 nmol mg^{-1} min^{-1}. This might indicate that (temporary) MoFe complex formation induces core structural rearrangements that substantially increase the ATPase activity of $(ChlL)_2$. When compared with the wild type, the reductase variant Y127D revealed much higher basal activity of 6.5 nmol mg^{-1} min^{-1}. Clearly, substitution of Tyr127 by aspartate held the sole reductase in a more active ATPase status. Consequently, this value was not increased upon the addition of $(ChlN/ChlB)_2$ or MoFe, as indicated by a specific activity of 5.9 or 5.8 nmol mg^{-1} min^{-1}, respectively. These findings also support the observation that protein–protein interactions of $(ChlL)_2$ Y127D with $(ChlN/ChlB)_2$ or MoFe are completely abolished.

The Y127S variant of $(ChlL)_2$ only showed a minor increase in the basal ATPase rate to 1.4 nmol mg^{-1} min^{-1}, relative to the wild-type reductase. The activity of this variant was not altered upon the addition of $(ChlN/ChlB)_2$. However, experiments in the presence of MoFe resulted in a significant increase of the ATPase activity to 6.1 nmol mg^{-1} min^{-1}. Substitution of Tyr127 by serine resulted in clear modulation of the ATPase activity in response to MoFe. In line with the nucleotide-dependent affinity changes depicted in Figure 6, we propose that this variant not only facilitates the nucleotide-dependent interaction with MoFe, but also allows for the triggering of ATPase activity in response to the chimeric protein–protein interaction. In summary, the single exchange of amino acid Tyr127 allowed for the alteration of the specificity of $(ChlL)_2$, while retaining partial functionality of the dynamic switch mechanism of DPOR and nitrogenase. According to these findings, the Y127S variant might be regarded as an initial step towards an alternative nitrogenase reductase.

Conclusions

We have described the chimeric interaction of nitrogenase-like reductases $(CfbC)_2$, $(ChlL)_2$, and related variants with the catalytic MoFe subunit of nitrogenase. Although the investigated reductases were unable to support nitrogenase activity, $(CfbC)_2$ and $(ChlL)_2$ were both able to engage in chimeric interactions with MoFe. However, for the wild-type reductases, the observed interaction was not differentially modulated by nucleotides; which is considered to be a prerequisite for nitrogenase function. By contrast, the binding affinity of the $(ChlL)_2$ variant Y127S was affected in the presence of different nucleotides. Moreover, in response to the binding of MoFe, the ATPase activity of this variant of $(ChlL)_2$ was activated, as also described for the homologous nitrogenase[11,45–49] or DPOR system.[23] Based on our mutagenesis results, we can conclude that tyro-

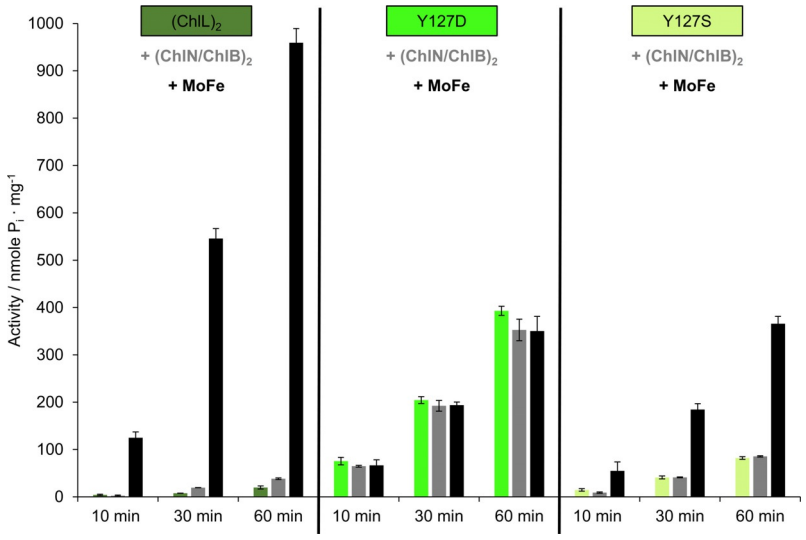

Figure 7. Reductant-independent ATPase activity of $(ChlL)_2$ or variants Y127D and Y127S. Basal ATPase activity of $(ChlL)_2$ (dark green), variant Y127D (bright green), and variant Y127S (yellow–green). ATPase activity of reductases in the presence of $(ChlN/ChlB)_2$ (gray) or MoFe (black). Mean values of three independent experiments with standard deviation are shown.

sine 127 is a central part of the chimeric docking interface and argue for a spatially related protein–protein interplay upon comparing the homologous DPOR and nitrogenase systems. But what is the possible contribution of nitrogenase-like proteins to the field of nitrogenase research? The Fe protein was recently appreciated as "an unsung hero of nitrogenase,"[5] since $(NifH)_2$ not only works as the obligate redox partner of MoFe during dinitrogen reduction, but also fulfills multiple roles during the reductive formation of the P-cluster and during the insertion of Mo and homocitrate upon FeMoco maturation.[50–52] The P-cluster is assembled at its target location in $(NifD/NifK)_2$ in a stepwise process, whereas FeMoco is assembled on the heterotetrameric scaffold, $(NifE/NifN)_2$, before it is finally translocated onto $(NifD/NifK)_2$. During both processes, $(NifH)_2$ serves as an ATP-dependent reductase, while inducing significant conformational changes of $(NifD/NifK)_2$.[52] The diverse functions of $(NifH)_2$ within the different stages of nitrogenase maturation rely on a set of as-yet uncharacterized protein–protein interactions. For the further understanding of the $(NifH)_2$-triggered processes, the trapping of individual states (e.g., of a $(NifH)_2/(NifE/NifN)_2$ complex) followed by structural analyses would be an important step towards the molecular understanding of nitrogenase maturation. Aside from this, nitrogenase-like reductases (e.g., $(ChlL)_2$ Y127S) might serve as a platform for the future development of a more-oxygen-tolerant nitrogenase reductase.

Experimental Section

Protein production and purification: CfbC from *M. barkeri* strain Fusaro DSM804 was heterologously produced and purified as described elsewhere.[31] *P. marinus* $(ChlL)_2$ and related variants Y127D and Y127S were produced in *Escherichia coli* as an N-terminal GST fusion protein and affinity purified mainly as reported in the literature.[38,53] *P. marinus* $(ChlN/ChlB)_2$ was bicistronically overproduced in *E. coli* and affinity purified by means of GST affinity chromatography. The untagged complex was released from the column by PreScission protease (GE Healthcare) treatment.[38,53] Untagged MoFe protein from *A. vinelandii* was purified as detailed elsewhere.[54] Protein purification and all subsequent analyses were performed under strict anaerobic conditions in an anaerobic chamber (Coy Laboratory Products).

Determination of protein concentration: The Bradford assay (Sigma) was used to determine the concentration of purified proteins.[55] Assays were performed according to the manufacturer's instructions by using bovine serum albumin (Carl Roth) as a standard.

Nucleotide-dependent interaction of reductases with the MoFe protein: The chimeric interaction between $(CfbC)_2$ and MoFe (as well as the homologous interaction with $(CfbD)_2$) was analyzed in ultrafiltration experiments by using Amicon ultrafiltration units with cellulose membranes (Merck Millipore) with a molecular-weight cutoff of 100 kDa. An excess of the reductase component was mixed with either MoFe or $(CfbD)_2$ in anaerobic buffer RP (50 mM Tris·HCl pH 8, 150 mM NaCl, 10 mM $MgCl_2$, 10% (*v/v*) glycerol) containing freshly added sodium dithionite (2 mM). In some experiments, the mixture was additionally supplemented with 1.5 mM ATP, ADP, or AMP-PNP. After incubation at 30 °C for 1 h, the mixtures were concentrated by ultrafiltration followed by dilution. This procedure was repeated three times. The proteins retained by the filter (stoichiometric amounts of $(CfbC)_2$ and $(CfbD)_2$ or MoFe) were analyzed by means of SDS-PAGE. Control experiments under identical conditions showed that noncomplexed proteins (smaller than 100 kDa) completely passed through the cellulose membrane.

The nucleotide-dependent interaction of GST-tagged $(ChlL)_2$ (or of variants Y127D and Y127S) with the MoFe protein was studied by immobilizing 2 nmol of the respective reductase component on glutathione agarose resin (0.3 mL; Macherey–Nagel), previously equilibrated in the presence of buffer A (100 mM HEPES pH 7.5, 150 mM NaCl, 10 mM $MgCl_2$). Subsequently, 2.5 nmol MoFe protein in buffer A (450 μL) containing 10 mM ATP, 10 mM ADP, 10 mM ADP·AlF_4^-, or 1.5 mM AMP-PNP was added (the formation of MgADP·AlF_4^- is reported in ref. [43]). Following 15 min incubation, unbound proteins were removed by using washing steps of 3× 0.5 mL and 1×1 mL buffer A containing the respective nucleotide or nucleotide analogue. PreScission protease treatment (GE Healthcare, 2 U, 17 h, 17 °C) allowed for the liberation of the bait protein. Resulting elution fractions were analyzed by means of SDS-PAGE. Band intensities of bait and prey proteins after Coomassie Blue staining were analyzed by means of densitometry with GelQuant.NET software (BiochemLabSolutions), taking into account the molecular weight of individual subunits. All results were reproduced in three independent experiments.

Native molecular weight of protein complexes: The native molecular weight of protein complexes (6.2 μM, 800 μL sample) was analyzed by means of gel permeation chromatography on a HiLoad Superdex 200 16/60 column (GE Healthcare) operated under strict anaerobic conditions in an anaerobic chamber (Coy Laboratory Products). The column was previously calibrated in the presence of buffer A by using marker proteins β-amylase (M_r = 200 000), albumin (M_r = 66 000), carbonic anhydrase (M_r = 29 000), and cytochrome *c* (M_r = 12 400) (Sigma–Aldrich) at a flow rate of 1.0 mL min^{-1}. Eluate absorption was monitored (λ = 280/420 nm) and fractions of 5 mL were examined by means of SDS-PAGE and Coomassie Blue staining.

The native molecular weight of complexes formed with $(CfbC)_2$ was determined on a Superdex 200 5/150 GL column (GE Healthcare) equilibrated with anaerobic buffer RP (10 μL samples, $(CfbC)_2/(CfbD)_2$: 15 μM/17.5 μM, $(CfbC)_2$/MoFe: 20 μM/6.5 μM, flow rate 0.3 mL min^{-1}, absorption at λ = 280/410 nm). The column was calibrated with marker proteins thyroglobulin (M_r = 670 000), γ-globulin (M_r = 158 000), ovalbumin (M_r = 44 000), and myoglobin (M_r = 17 000).

Reductant-independent ATPase activity of $(ChlL)_2$: Specific ATPase activity of $(ChlL)_2$ and variants Y127D and Y127S at a concentration of 1 μM was analyzed in buffer A (200 μL). Modulation of this reductant-independent ATPase activity in the presence of catalytic components $(ChlN/ChlB)_2$ or MoFe (0.5 μM) was investigated. For subsequent ATPase activity assays, the purification of $(ChlN/ChlB)_2$, $(ChlL)_2$, and variants Y127D and Y127S was modified by an additional pre-elution step in the presence of 10 mM ATP. A typical assay at 25 °C was initiated by the addition of 10 mM ATP (10 μL). After 10, 30, and 60 min, reactions were stopped and the amount of free phosphate was quantified by using the PiColorLock phosphate detection reagent (Expedeon), according to the manufacturer's instructions. The freshly prepared detection reagent (50 μL) was mixed with each assay solution (200 μL) and the absorption of the resulting malachite green complex was determined at a wavelength of 600 nm by using a microplate spectrophotometer (Thermo Scientific Multiskan GO). In all cases, control reactions

in the absence of individual protein components or in the absence of ATP were performed. All experiments were performed in triplicate.

Acknowledgements

This work was funded by the Deutsche Forschungsgemeinschaft with grants to J.M. (MO1749/2-1), G.L. (LA2412/6-1), and O.E. (El520/10), as part of the Priority Programme SPP1927 Iron-Sulfur for Life, and with grant RTG 1976 to O.E. (Research Training Group).

Conflict of Interest

The authors declare no conflict of interest.

Keywords: enzyme catalysis · metalloproteins · nitrogenases · nitrogen fixation · protein–protein interactions

[1] B. K. Burgess, D. J. Lowe, *Chem. Rev.* **1996**, *96*, 2983 – 3012.
[2] V. Smil, *Enriching the Earth: Fritz Haber, Carl Bosch, and the Transformation of World Food Production*, MIT Press, Cambridge, **2004**.
[3] M. M. Georgiadis, H. Komiya, P. Chakrabarti, D. Woo, J. J. Kornuc, D. C. Rees, *Science* **1992**, *257*, 1653 – 1659.
[4] L. Chen, N. Gavini, H. Tsuruta, D. Eliezer, B. K. Burgess, S. Doniach, K. O. Hodgson, *J. Biol. Chem.* **1994**, *269*, 3290 – 3294.
[5] A. J. Jasniewski, N. S. Sickerman, Y. Hu, M. W. Ribbe, *Inorganics* **2018**, *6*, 25.
[6] J. B. Howard, D. C. Rees, *Annu. Rev. Biochem.* **1994**, *63*, 235 – 264.
[7] W. N. Lanzilotta, M. J. Ryle, L. C. Seefeldt, *Biochemistry* **1995**, *34*, 10713 – 10723.
[8] M. J. Ryle, L. C. Seefeldt, *Biochemistry* **1996**, *35*, 4766 – 4775.
[9] L. C. Seefeldt, D. R. Dean, *Acc. Chem. Res.* **1997**, *30*, 260 – 266.
[10] F. A. Tezcan, J. T. Kaiser, D. Mustafi, M. Y. Walton, J. B. Howard, D. C. Rees, *Science* **2005**, *309*, 1377 – 1380.
[11] L. C. Seefeldt, B. M. Hoffman, D. R. Dean, *Annu. Rev. Biochem.* **2009**, *78*, 701 – 722.
[12] B. M. Hoffman, D. Lukoyanov, Z. Y. Yang, D. R. Dean, L. C. Seefeldt, *Chem. Rev.* **2014**, *114*, 4041 – 4062.
[13] I. Djurdjevic, O. Einsle, L. Decamps, *Chem. Asian J.* **2017**, *12*, 1447 – 1455.
[14] T. M. Buscagan, D. C. Rees, *Joule* **2019**, *3*, 2662 – 2678.
[15] L. C. Seefeldt, J. W. Peters, D. N. Beratan, B. Bothner, S. D. Minteer, S. Raugei, B. M. Hoffman, *Curr. Opin. Chem. Biol.* **2018**, *47*, 54 – 59.
[16] R. Y. Igarashi, L. C. Seefeldt, *Crit. Rev. Biochem. Mol. Biol.* **2003**, *38*, 351 – 384.
[17] S. Burén, L. M. Rubio, *FEMS Microbiol. Lett.* **2018**, *365*, fnx274.
[18] F. Moshiri, B. R. Crouse, M. K. Johnson, R. J. Maier, *Biochemistry* **1995**, *34*, 12973 – 12982.
[19] J. Schlesier, M. Rohde, S. Gerhardt, O. Einsle, *J. Am. Chem. Soc.* **2016**, *138*, 239 – 247.
[20] Y. Fujita, C. E. Bauer, *J. Biol. Chem.* **2000**, *275*, 23583 – 23588.
[21] M. G. Duyvis, H. Wassink, H. Haaker, *FEBS Lett.* **1996**, *380*, 233 – 236.
[22] J. Moser, C. Lange, J. Krausze, J. Rebelein, W. D. Schubert, M. W. Ribbe, D. W. Heinz, D. Jahn, *Proc. Natl. Acad. Sci. USA* **2013**, *110*, 2094 – 2098.
[23] M. J. Bröcker, D. Wätzlich, M. Saggu, F. Lendzian, J. Moser, D. Jahn, *J. Biol. Chem.* **2010**, *285*, 8268 – 8277.
[24] R. Sarma, B. M. Barney, T. L. Hamilton, A. Jones, L. C. Seefeldt, J. W. Peters, *Biochemistry* **2008**, *47*, 13004 – 13015.
[25] M. J. Bröcker, S. Schomburg, D. W. Heinz, D. Jahn, W. D. Schubert, J. Moser, *J. Biol. Chem.* **2010**, *285*, 27336 – 27345.
[26] N. Muraki, J. Nomata, K. Ebata, T. Mizoguchi, T. Shiba, H. Tamiaki, G. Kurisu, Y. Fujita, *Nature* **2010**, *465*, 110 – 114.
[27] *The PyMOL Molecular Graphics System*, Version 2.0, Schrödinger, LLC.
[28] W. L. Ellefson, W. B. Whitman, R. S. Wolfe, *Proc. Natl. Acad. Sci. USA* **1982**, *79*, 3707 – 3710.
[29] H. C. Friedmann, A. Klein, R. K. Thauer, *FEMS Microbiol. Rev.* **1990**, *7*, 339 – 348.
[30] G. Färber, W. Keller, C. Kratky, B. Jaun, A. Pfaltz, C. Spinner, A. Kobelt, A. Eschenmoser, *Helv. Chim. Acta* **1991**, *74*, 697 – 716.
[31] S. J. Moore, S. T. Sowa, C. Schuchardt, E. Deery, A. D. Lawrence, J. V. Ramos, S. Billig, C. Birkemeyer, P. T. Chivers, M. J. Howard, S. E. Rigby, G. Layer, M. J. Warren, *Nature* **2017**, *543*, 78 – 82.
[32] K. Zheng, P. D. Ngo, V. L. Owens, X.-p. Yang, S. O. Mansoorabadi, *Science* **2016**, *354*, 339.
[33] E. S. Boyd, J. W. Peters, *Front. Microbiol.* **2013**, *4*, 201.
[34] D. W. Emerich, R. H. Burris, *J. Bacteriol.* **1978**, *134*, 936 – 943.
[35] T. A. Clarke, S. Maritano, R. R. Eady, *Biochemistry* **2000**, *39*, 11434 – 11440.
[36] D. W. Emerich, R. H. Burris, *Proc. Natl. Acad. Sci. USA* **1976**, *73*, 4369 – 4373.
[37] D. W. Emerich, T. Ljones, R. H. Burris, *Biochim. Biophys. Acta* **1978**, *527*, 359 – 369.
[38] D. Wätzlich, M. J. Bröcker, F. Uliczka, M. Ribbe, S. Virus, D. Jahn, J. Moser, *J. Biol. Chem.* **2009**, *284*, 15530 – 15540.
[39] C. P. Owens, F. E. H. Katz, C. H. Carter, M. A. Luca, F. A. Tezcan, *J. Am. Chem. Soc.* **2015**, *137*, 12704 – 12712.
[40] P. L. Searle, *Analyst* **1984**, *109*, 549 – 568.
[41] L. C. Seefeldt, S. A. Ensign, *Anal. Biochem.* **1994**, *221*, 379 – 386.
[42] P. Csermely, R. Palotai, R. Nussinov, *Trends Biochem. Sci.* **2010**, *35*, 539 – 546.
[43] J. Moser, G. Layer in *Metalloproteins: Methods and Protocols* (Ed.: Y. Hu), Springer, New York, **2019**, pp. 25 – 35.
[44] L. C. Seefeldt, B. M. Hoffman, J. W. Peters, S. Raugei, D. N. Beratan, E. Antony, D. R. Dean, *Acc. Chem. Res.* **2018**, *51*, 2179 – 2186.
[45] J. Cordewener, A. ten Asbroek, H. Wassink, R. Eady, H. Haaker, C. Veeger, *Eur. J. Biochem.* **1987**, *162*, 265 – 270.
[46] S. Imam, R. R. Eady, *FEBS Lett.* **1980**, *110*, 35 – 38.
[47] D. Y. Jeng, J. A. Morris, L. E. Mortenson, *J. Biol. Chem.* **1970**, *245*, 2809 – 2813.
[48] C. Larsen, S. Christensen, G. D. Watt, *Arch. Biochem. Biophys.* **1995**, *323*, 215 – 222.
[49] T. Ljones, R. H. Burris, *Biochim. Biophys. Acta* **1972**, *275*, 93 – 101.
[50] Y. Hu, M. C. Corbett, A. W. Fay, J. A. Webber, K. O. Hodgson, B. Hedman, M. W. Ribbe, *Proc. Natl. Acad. Sci. USA* **2006**, *103*, 17119 – 17124.
[51] Y. Hu, M. C. Corbett, A. W. Fay, J. A. Webber, K. O. Hodgson, B. Hedman, M. W. Ribbe, *Proc. Natl. Acad. Sci. USA* **2006**, *103*, 17125 – 17130.
[52] C. C. Lee, M. A. Blank, A. W. Fay, J. M. Yoshizawa, Y. Hu, K. O. Hodgson, B. Hedman, M. W. Ribbe, *Proc. Natl. Acad. Sci. USA* **2009**, *106*, 18474 – 18478.
[53] M. J. Bröcker, D. Wätzlich, F. Uliczka, S. Virus, M. Saggu, F. Lendzian, H. Scheer, W. Rüdiger, J. Moser, D. Jahn, *J. Biol. Chem.* **2008**, *283*, 29873 – 29881.
[54] T. Spatzal, M. Aksoyoglu, L. Zhang, S. L. Andrade, E. Schleicher, S. Weber, D. C. Rees, O. Einsle, *Science* **2011**, *334*, 940.
[55] M. M. Bradford, *Anal. Biochem.* **1976**, *72*, 248 – 254.

Manuscript received: December 16, 2019
Revised manuscript received: January 17, 2020
Accepted manuscript online: January 20, 2020
Version of record online: February 27, 2020